euronoise

Numerical prediction of interaction between combustion, acoustics and vibration in gas turbines

Artur Pozarlik and Jim Kok

University of Twente, P.O. Box 217, 7500 AE Enschede, Netherlands
a.k.pozarlik@utwente.nl

The turbulent flame in the lean combustion regime in a gas turbine combustor generates significant thermo-acoustic instabilities. The flame can amplify fluctuations in the released heat, and thus in the acoustic field as well. The induced pressure oscillations will drive vibrations of the combustor walls and burner parts. Stronger fluctuating pressure results in stronger fluctuations in the wall structure. Due to fatigue the remaining life time of the hardware will be reduced significantly. This paper investigates the modeling of acoustic oscillations and mechanical vibrations induced by turbulent lean premixed natural gas combustion. The mutual interaction of the combustion processes, induced oscillating pressure field in the combustion chamber, and induced vibration of the liner walls are investigated with numerical techniques. A partitioned procedure is used here: CFX-11 for the CFD analysis and Ansys-11 for the CSD analysis are coupled to give insight into a correlation between acoustic pressure oscillations and liner vibrations. These results will be compared with the available experimental data. The data are gathered in a purpose built 500 kW/5 bar premixed natural gas test rig.

1 Introduction

A major part of the electric power for domestic and industrial use is produced by natural gas fired gas turbines. To reduce their emission of nitric oxide, gas turbine technology evolves to low burning temperatures by introduction of lean premixed natural gas combustion. However, in gas turbines operated in the lean premixed natural gas combustion regime, combustion instabilities related to noise feed back, can occur. The instabilities are driven by a source related to the interaction between heat and sound [5,13,14]. The unsteady heat release is an acoustic source and leads to pressure wave generation. When Rayleigh's criterion [18] (extended in [16]) is fulfilled, i.e. the oscillations in heat release and pressure variations are in phase, and the energy gain exceeds the losses in the acoustic domain, a self-excited loop is created (Eq.1). The combustion instabilities will grow exponentially until they reach a saturation limit.

$$\frac{(\gamma-1)}{\gamma p_0}\int_V \int_0^\tau p'Q'dtdV > \int_A \int_0^\tau p'\boldsymbol{u}dtdA \qquad (1)$$

The induced pressure oscillations will induce vibrations of the combustor walls and burner parts. Due to fatigue, the remaining life time of the hardware can be reduced significantly [3,19]. The processes to be investigated are composed of two weakly coupled mechanisms. One mechanism consists of the acoustic feedback loop. Here the combustor can be seen as an acoustically closed resonator, where the flame inside it is a source of noise [8]. The flame and the acoustics are coupled through the aerodynamics of the combustion flow. The other mechanism consists of the liner wall, which is thin and flexible and damped with respect to vibration only by the cooling flow enveloping it. The liner wall is driven into vibration due to differential pressure oscillations and the liner velocities can reach high amplitudes due to the very low damping. These processes were investigated experimentally in the DESIRE test rig at the University of Twente [9,11]. This provided data for numerical code validation. The main investigated case has the following operation characteristics: pressure 1.5 bar; thermal power 125 kW with air factor 1.8 in lean premixed natural gas combustion. Computational Fluids models have been developed for the flame behaviour, the aerodynamics and the acoustics inside the combustor. These models were operated in combination with structural models for the vibrational behaviour of the combustor liner. The combined result represents the behaviour of the two structural systems coupled to the combustor fluid system.

2 Experiment

In order to measure vibration of the liner during the combustion process, the setup available at the University of Twente (Fig.1) is equipped with a system of pressure casing windows. This transparent system allows optical measurements of the liner velocity. The velocity amplitude is obtained with the use of a Polytec Laser Doppler Vibrometer. A flexible section with a thickness much smaller than the major part of the liner is located directly behind the transparent window. This thin, flexible section responds stronger to any changes in the pressure field inside the combustion chamber during the transient combustion.

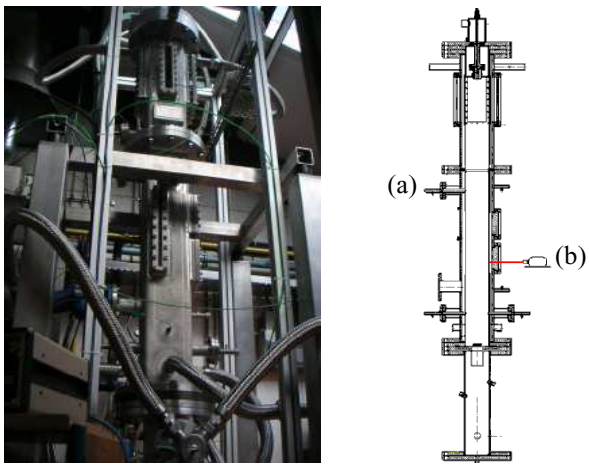

Fig. 1. Experimental setup with data recording points: (a) pressure, (b) velocity

To prevent changes in the vibration pattern, there are no pressure sensors, thermocouples or other measurement equipments attached to the flexible wall. The data from the pressure sensor closest to the flexible wall is here presented. This sensor is located on the stiff part of the liner, about 0.5 m above the point where vibrations are collected (Fig.1). The drawback of this solution is that the exact pressure fluctuations at the point of vibration measurements are unknown.

The forced oscillations are investigated here. In this case, the fuel to air equivalence ratio is oscillated with frequency 300 Hz and amplitude 8.5% of the mean.

The results of the experiment are compared with the numerical data at conditions depicted in (Tab.1).

Power	Abs. pressure	Air factor	Mass flow rate	Air preheats. temperature
125 [kW]	1.5 [bar]	1.8 [-]	75.53 [g/s]	573 [K]

Tab. 1. Operation conditions used for experiment and numerical simulations

3 One-way interaction

Numerical simulations of fluid structure interaction problems can be found in many engineering and scientific applications [10,12]. In this work, the case in (Tab.1) is investigated. During lean premixed combustion three main phenomena i.e. combustion, acoustics and vibration interact and influence the system behaviour. To investigate the combustion, two approaches for resolving fluid structure interaction are combined. For both, the CFD analysis is performed, followed by further investigation with the use of FEM (Fig.2).

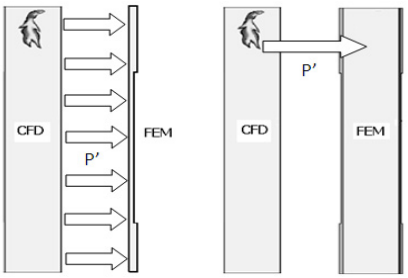

Fig. 2. One-way interaction (left) and acousto-elastic analysis (right)

The first approach is the one way interaction, which is based on direct coupling the reacting flow with the liner vibrations (Fig.2-left). Unlike the monolithical approach [2], where the fluid and structural equations are solved in a single computational domain, the partitioned procedures [6,7] use independent techniques for the fluid and structure subdomains and exchange data along the fluid structure interface. The partitioned approach can thus take full advantage of existing, well developed and tested codes for fluid and structure analysis. Two commercial codes from Ansys, i.e. CFX 11 [4] for the reacting flow calculations and Ansys 11 FEM package [1] for the structural analysis are used here. Exchange of information between CFX and Ansys is possible with the use of the MFX coupling code, available within the Ansys FEM package. In this work, we are interested in transferring the boundary conditions (pressure) from the CFD code to the CSD code through the interface connection available between the codes.

The concept of the dynamical exchange of data between the fluid and the structural domain through the interface connection used here is reduced to one way interaction. As the liner available at the University of Twente is stiff, it is difficult to induce high fluctuation amplitudes in the pressure field inside the combustion chamber and at the same time the mass of the fluctuating air/exhaust gases is too low to induce higher structural vibration. Thus applied here, the one way assumption is a good approximation and no information on the structural displacement needs to be sent back to the CFX code. In the structural code, the dynamical analysis of the liner vibration is done according to the linear theory:

$$[M]\{\ddot{U}\} + [C]\{\dot{U}\} + [K]\{U\} = \{F(t)\} \qquad (2)$$

[M] is the structural mass matrix; [C] is the structural damping matrix; [K] the structural stiffness matrix; $\{\ddot{U}\}$ the acceleration vector; $\{\dot{U}\}$ the velocity vector; {U} the displacement vector; {F(t)} the time dependent load vector. To assure lossless transfer of mechanical loads on the fluid structure interface, the shearing information faces must have the same dimensions and global coordinates. The data transfer between faces that are separated, rotated or have significantly different geometry is not possible. Information about forces is shared every time step.

3.1 CFD models

The URANS numerical approach is used for combustion flow prediction. Polifke et al. [17] and van Kampen [11] have already shown that it is possible to resolve the acoustics wave inside URANS. Resolving the time accurate compressible Navier-Stokes equations for acoustics demands accurate time step and mesh resolution. To save computation time and to increase the number density of elements within the calculated domain, the computational domain was reduced to a quarter section of the real combustion chamber, with periodic boundary conditions. A total number of 720 000 unstructured elements, mostly placed in the flame and recirculation region are used for calculations. The near-wall region is created with the use of prism elements to avoid generating highly distorted tetrahedral elements at the face. The volume average CFL number (Eq.3) during transient calculations for a time step 1e-4 s was equal to 20. The CFX code is an implicit scheme thus it is stable even during calculations with high CFL numbers. Previous investigations using a simplified geometry with the same mesh resolution but various time steps, with CFL number equal to 0.1 - 10, showed a minor influence on the obtained pressure field inside the combustion chamber (Fig.3).

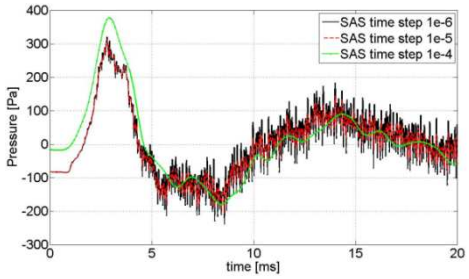

Fig. 3. Instantaneous pressure changes at the location of the pressure recording point for three different time steps

$$CFL = (u + c)\Delta t/\Delta x \qquad (3)$$

To reduce the computational effort, calculations with the highest CFL number are performed. The combustion processes are modelled with the use of the Eddy Dissipation/Finite Rate Chemistry combustion model [4]. This way, the reaction rate at each step is limited by turbulent mixing or chemical kinetics. Standard the k-ε model or the SAS-SST model as available in the CFX

code are used to resolve turbulence. The concept of SAS simulation is based on the introduction of the von Karman length-scale into the turbulence scale equations. Therefore the SAS-SST models can dynamically change and adjust to resolved structures, which results in behaviour similar to LES calculations in unsteady regions of the flow field [15]. Previous calculations show that the SAS-SST model is less dissipative for acoustic energy than the commonly used standard k-ε turbulent model.
The velocity and turbulence profiles at the inlet are taken from the steady-state calculations of the full setup geometry. The static average pressure is imposed at the combustion chamber outlet. On the investigated wall, a heat transfer coefficient is imposed. Other walls have adiabatic and no-slip conditions. The influence of the pressure from the cooling passage is neglected. The investigated flame is a premixed natural gas flame under conditions presented in (Tab.1). The total calculation time was equal to 80 ms for the SAS-SST, and 100 ms for the k-ε turbulence model.

3.2 CSD model

In parallel with the CFD simulation, the transient structural displacements of the liner wall are computed. As a result of the modular liner design, no significant thermal stresses are generated. Therefore, calculations are performed for the typical liner temperature during operating conditions, which is equal to 760°C. Moreover, the liner model is reduced to a one liner wall without the sliding connection and holes for thermocouples and pressure transducers. The wall has fixed support on all four sides (Fig.4). Material properties of stainless steel 310 at the operational temperature, together with geometrical dimensions of the wall are depicted in (Tab.2).

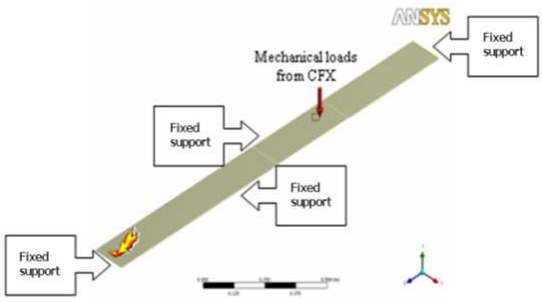

Fig. 4. Boundary conditions used for CSD calculation

Total length	Wall width	Stiff part thickness	Flexible part length
1.813 [m]	0.15 [m]	0.004 [m]	0.4 [m]
Flexible part thickness	Material density	Young's modulus	Poisson's ratio
0.0015 [m]	7844 [kg/m^3]	138 [GPa]	0.3 [-]

Tab. 2. Geometrical dimensions and material properties of the liner

Mechanical loads from the CFX calculation are transferred to the internal liner face. A total number of 19 000 uniformly distributed SOLID92 tetrahedral elements is used for the dynamic calculation. Time step and total calculation time are the same as in the CFD calculation.

4 Acousto-elastic interaction

The direct prediction of the mid and far field acoustics by the CFD computation is difficult to achieve, mainly due to requirements of meshing and time step. The CFD mesh must span all the way to the reception points with enough spatial resolution to directly resolve acoustic waves over the propagation distance with minimal to no numerical damping. These requirements are discouraging to resolve acoustic directly in CFD codes.
The geometrical dimensions of the combustion chamber investigated here, make the distance propagated by a wave relatively high. Therefore numerical dissipation and dispersion has influence on the results. The longer the propagation distance and the higher the frequencies involved the more significant influence of these two effects is observed.

In order to reduce errors introduced by numerical dissipation and dispersion, the CFD domain is truncated near the acoustics source (flame). It is assumed that the acoustic wave at the place of truncation is not significantly changed. This way the numerical domain is divided in two regions, namely, the near field acoustics in the vicinity of the flame and the far field acoustics in far distance from the acoustic source. The near field acoustics play a key role in prediction and production of the far field noise. At first by using a time accurate solution of the compressible Navier-Stokes equations, the near filed noise is predicted. Later, the results are imported to the FEM code (Fig.2-right) where the homogenous wave equation is solved. Using the Galerkin procedure after some manipulation and taking into account dissipation of energy due to damping present at the fluid boundary eq.4 is obtained.

$$\int_V \delta P \frac{1}{c^2}\frac{\partial^2 P}{\partial t^2} dV - \int_V \delta P \{L\}^T (\{L\}P) dV + \int_S \delta P \left(\frac{r}{\rho_0 c}\right)\frac{1}{c}\frac{\partial P}{\partial t} dS = 0 \qquad (4)$$

$$and: \nabla \cdot (\ \ ) = \{L\}^T = \left[\frac{\partial}{\partial x} \quad \frac{\partial}{\partial y} \quad \frac{\partial}{\partial z}\right] \ and \quad \nabla(\ \ ) = \{L\}$$

Where: r is the characteristic impedance, ρ_0 is the mean fluid density, c is the speed of sound, P is the acoustic pressure P(x,y,z,t), V is the volume of the domain and S is the surface [1].
The FEM code used for the acousto-elastic interaction includes not only acoustic elements which are responsible for correct resolving of acoustic pressure waves travelling along the chamber but it is also equipped with the solid elements which serve to resolve the displacements and stresses inside the investigated walls.
The interaction of the fluid at the mesh interface causes the acoustic pressure to exert a force applied to the structure and the structural motion to produce an effective fluid load. The governing finite element matrix equations then become:

$$\begin{bmatrix} M_S & 0 \\ \rho_0 R^T & M_F \end{bmatrix}\begin{bmatrix} \ddot{U} \\ \ddot{P} \end{bmatrix} + \begin{bmatrix} K_S & -R \\ 0 & K_F \end{bmatrix}\begin{bmatrix} U \\ P \end{bmatrix} = \begin{bmatrix} F_S \\ F_F \end{bmatrix} \qquad (5)$$

[R] is a coupling matrix that represents the effective surface area associated with each node on the fluid structure

interface. F_S and F_F are structural and fluid forces, respectively.
Both the structural and fluid load quantities that are produced at the fluid structure interface are functions of unknown nodal degrees of freedom.

In order to model the fluid structure interaction inside the FEM code, three different types of elements are used. For the structure, SHELL63 elements with the element real constant equal to the thickness of the respective section are used. The air cavity of the combustion chamber is modelled using the FLUID30 acoustic elements. One layer of the FLUID30 elements with ability to recognize structure on one side and fluid on the other is included between the structural and fluid elements. This configuration assures correct transfer of loads between the acoustic fluid and the liner wall. Similarly to the previous calculations, only the combustion chamber and the liner are resolved. The pressure changes from the SAS-SST calculations are taken from the near flame region and are implemented to the acousto-elastic model. The geometry is simplified to the rectangular shape without the exhaust pipe. Term $\beta=r/(\rho_n c)$ is calculated based on change in the cross-section area and imposed as the outlet boundary conditions. At the inlet, an acoustically hard wall is imposed. The model includes all four liner walls. Material properties of the stainless steel and the temperature field inside the combustion chamber are the same as in the one way interaction analysis. The speed of sound for acoustic elements is prescribed according to the average temperature field obtained in the CFD calculation.

5 Results

Comparison of the experimental data and the numerical results is done for the pressure and velocity amplitude and frequency.
Numerical results of the pressure oscillations as a function of time inside the combustion chamber, obtained during both numerical investigations present significant under-prediction of the pressure amplitude (Fig.5). Only at the beginning of calculations, experiment and acousto-elastic analysis are in good agreement. Thereafter, significant decrease in the pressure amplitude is observed.

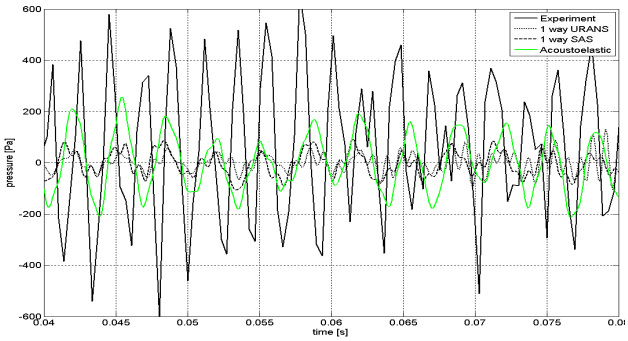

Fig.5. Pressure changes

Similarly, the frequency of the pressure changes differs from the experimental data. The low frequency instabilities (below 200 Hz) are not visible in the experiment, and they are more likely to be the result of numerical error. Above 200 Hz, all models predicted correctly the forcing peak at 300 Hz. Moreover, the one way interaction with the use of the SAS-SST model and the acousto-elastic analysis show a peak at the frequency of the instabilities, around 450 Hz. The instability is also predicted by the k-ε model, but the amplitude of the peak is significantly lower with comparison to the experimental one (Fig.6). The acousto-elastic model presents also instabilities around 630 Hz, which match well with experimental data.
Vibrations in the combustion system are directly coupled to the self-excited loop of the thermo-acoustic instabilities. The amplitude of changes in the pressure field leads to high dynamical forces on the liner face, which finally induces strong fluctuations in the material. As a result of smaller fluctuations in the pressure field also the magnitude of the velocity change during vibrations is lower (Fig.7). However, the difference is not as significant as in the case of the pressure fluctuations. This discrepancy is more likely caused by damping which is present during the experiment and is not taken into account in the numerical simulation. Similar to the results of the pressure field, also here the best match exists between experimental data and the SAS-SST model and acousto-elastic interaction.

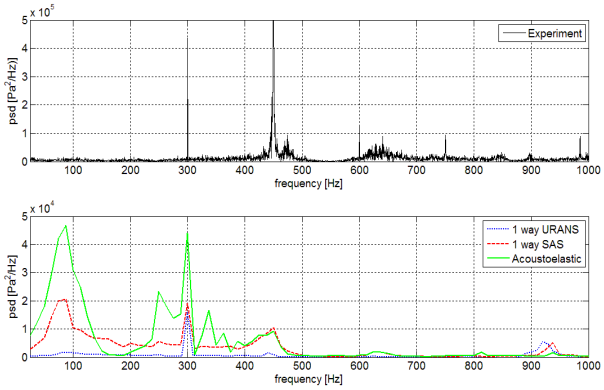

Fig. 6. Pressure spectrum

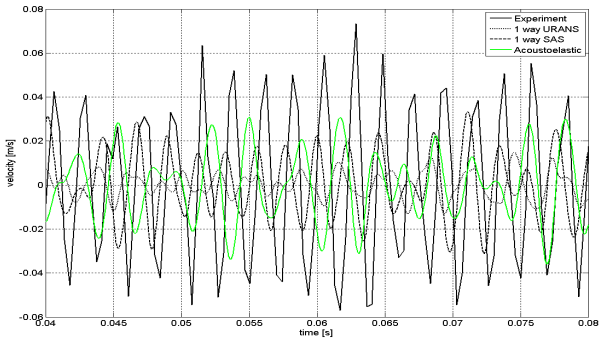

Fig. 7. Velocity fluctuations

Spectral analysis of the velocity field shows good agreement between experiments and all numerical models. Both, the forcing peak at 300 Hz and the one associated with the thermo-acoustic instabilities are predicted correctly. Also instabilities around 320 Hz are clearly visible (Fig.8). Moreover, in case of acousto-elastic analysis, higher order peaks are visible, as well.
All the above-mentioned discrepancies are most likely the consequence of multiple errors that combined together lead to the under-prediction of the measured oscillations. Some part of the acoustic energy is damped during flow through the combustion chamber by the numerical scheme used for the calculation. The mesh density has also direct influence

on the flame as it changes slightly the position of the flame and its length. The CFL number above unity is another factor of great importance. However, the correctly predicted frequencies of the instabilities suggest that it is possible to resolve acoustic wave in the CFD calculation. Improving all factors mentioned above should render more accurate results, but it entails much higher computational costs.

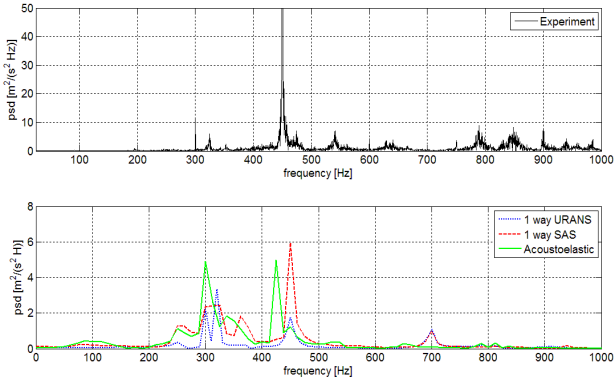

Fig.8. Velocity spectrum

6 Conclusion

Numerical investigation of the fluid structure interaction between reacting flow inside the combustion chamber, acoustics induced by the fluctuating flame and liner wall vibration has been performed. Two different fluid structure interaction models were used to predict amplitude of pressure and velocity fluctuations. Computations of the one way interaction with the use k-ε turbulence model show under-prediction of the numerical results compared to the results obtained during the experiment. It is caused by small changes in the acoustic pressure amplitude predicted by the CFD code and by disturbances in mutual influence between acoustic waves. In the aftermath of this discrepancy, also the amplitude of the velocity was under-predicted. The one way interaction based on the SAS-SST turbulence model and acousto-elastic interaction showed similar results. Both models under-predicted the amplitude of pressure changes, but hazardous frequencies were marked correctly. Analogous behaviour was observed in the case of the velocity field. However here, the velocity amplitude as a consequence of no physical damping included in analyses matched better with experimental data. The hazardous frequencies are marked correctly.

Acknowledgments

This work is performed in the EU sponsored project FLUISTCOM in the Marie Curie Program, contract number MRTN-CT-2003-504183. The authors would like to thank CFX-ANSYS for the use of the code.

References

[1] Ansys HTML Online Documentation, *Ansys 11.0,* Ansys Inc. 2007

[2] F.J. Blom, *A monolithical fluid-structure interaction algorithm applied to the piston problem,* Comput. Methods Appl. Engrg., 167, 369-391, 1998

[3] Breard, C., Sayma, A., Vahdati, M., & Imregun, M.. Aeroelasticity analysis of an industrial gas turbine combustor using a simplified combustion model. *Journal of Fluids and Structures , 16*, 1111-1126, 2002

[4] CFX-Ansys HTML Online Documentation, *CFX-Ansys 11.0,* Ansys Inc. 2007

[5] S. Decruix, T. Shuller, D. Durox, S. Candel, *Combustion Dynamics and Instabilities: Elementary Coupling and Driving Mechanisms,* Journal of Propulsion and Power, 19, No. 5, 722-733, 2003

[6] Farath, C., Lesoinne, M., & Le Tallec, P. Load and Motion transfer Algorithms for Fluid/Structure Interaction Problems with Non-Matching Descrete Interfaces: Momentum and Energy Conservation, Optimal Discretization and Application to Aeroelasticity. *Computer Methods in Applied Mechanics and Engineering , 157*, 95-114, 1998

[7] C.A. Fellipa, K.C. Park, C. Farhat, *Partitioned analysis of coupled mechanical systems,* Comput. Methods Appl. Engrg., 190, 3247-3270, 2001

[8] Hubbard, S., & Dowling, A., Acoustic Resonances of an Industrial Gas Turbine Combustion System. *Journal of Engineering for Gas Turbines and Power , 123*, 766-773, 2001

[9] R. Huls, *Acousto-Elastic Interaction in Combustion Chamber,* PhD thesis, University of Twente, Enschede, The Netherlands, 2006

[10] R.A. Huls, J.F. van Kampen, J.B.W. Kok, A. de Boer, *Fluid structure interaction to predict liner vibrations in an industrial combustion system,* Proceedings of 10th International Congress on Sound and Vibration (ICSV 10), Stockholm, Sweden, 2003

[11] J.F. van Kampen, *Acoustic pressure oscillations induced by confined turbulent premixed natural gas flames,* PhD thesis, University of Twente, Enschede, The Netherlands, 2006

[12] Khatir Z, Pozarlik A.K, Cooper R.K, Watterson J.W, Kok J.B.W, *Numerical study of coupled fluid-structure interaction for combustion system*, Proceedings of Conference on Numerical Methods for Fluid Dynamics, 16-29 March 2007, Reading, UK

[13] Lieuwen, T., Combustion Driven Oscillations in Gas Turbines. *Turbomachinery International , 44*, 16-18, 2003

[14] T. Lieuwen, H. Torres, C. Johnson, B.T. Zinn, *A Mechanism of Combustion Instability in Lean Premixed Gas Turbine Combustors,* Journal of Engineering for Gas Turbines and Power, 123, 182-189, 2001

[15] F. Menter, Y. Egorov, *Turbulence Modeling of Aerodynamic Flows,* Proceedings of International Aerospace CFD Conference, 18-19 June 2007, Paris, France

[16] Poinsot, T., Veynante, D., *Theoretical and Numerical Combustion* . R.T. Edwards, Inc., 2005

[17] Polifke W., Poncet A., Paschereit C.O., Döbbeling K., *Reconstruction of acoustic transfer matrices by instationary computational fluid dynamics,* Journal of Sound and Vibration, 245, 483-510, 2001.

[18] Rayleigh, J. (1878). The Explanation of Certain Acoustic Phenomena. *Nature, 18* , 319-321, 1878

[19] T. Tinga, J.F. van Kampen, B. de Jager, J.B.W. Kok, *Journal of Engineering for Gas Turbines and Power,* 129, 69-79, 2007